THE JOURNAL OF BIOLOGICAL CHEMISTRY VOL. 287, NO. 50, pp. 42064–42070, December 7, 2012

N-Sulfation of Heparan Sulfate Regulates Early Branching Events in the Developing Mammary Gland*

Received for publication, September 27, 2012 Published, JBC Papers in Press, October 11, 2012, DOI 10.1074/jbc.M112.423327

Kevin T. Bush[‡1], Brett E. Crawford[§¶1,2], Omai B. Garner[§¶2,3,4], Kabir B. Nigam[§4], Jeffrey D. Esko[§‖5], and Sanjay K. Nigam[‡§‡‡6]**

*From the Departments of [‡]Pediatrics, [§]Cellular and Molecular Medicine, [¶]Biomedical Sciences Graduate Program, [‖]Glycobiology Research and Training Center, **Medicine (Division of Nephrology and Hypertension), and [‡‡]Bioengineering, University of California, San Diego, La Jolla, California 92093*

Background: Mammary epithelial branching morphogenesis depends on proper sulfation of heparan sulfate proteoglycans.
Results: The absence of both *Ndst1* and *Ndst2* induces increased branching of the ductal epithelium.
Conclusion: *N*-Sulfation regulates primary and secondary branching events in the developing mammary gland.
Significance: Stages of ductal branching and lobuloalveolar formation are regulated by distinct sets of heparan sulfate biosynthetic enzymes.

Branching morphogenesis, a fundamental process in the development of epithelial organs (*e.g.* breast, kidney, lung, salivary gland, prostate, pancreas), is in part dependent on sulfation of heparan sulfate proteoglycans. Proper sulfation is mediated by biosynthetic enzymes, including exostosin-2 (Ext2), *N*-deacetylase/*N*-sulfotransferases and heparan sulfate *O*-sulfotransferases. Recent conditional knockouts indicate that whereas primary branching is dependent on heparan sulfate, other stages are dependent upon selective addition of *N*-sulfate and/or 2-*O* sulfation (Crawford, B .E., Garner, O. B., Bishop, J. R., Zhang, D. Y., Bush, K. T., Nigam, S. K., and Esko, J. D. (2010) *PLoS One* 5, e10691; Garner, O .B., Bush, K. T., Nigam, S .K., Yamaguchi, Y., Xu, D., Esko, J. D., and Nigam, S. K. (2011) *Dev. Biol.* 355, 394–403). Here, we analyzed the effect of deleting both *Ndst2* and *Ndst1*. Whereas deletion of *Ndst1* has no major effect on primary or secondary branching, deletion of *Ndst2* appears to result in a mild increase in branching. When both genes were deleted, ductal growth was variably diminished (likely due to variable Cre-recombinase activity), but an overabundance of branched structures was evident irrespective of the extent of gland growth or postnatal age. "Hyperbranching" is an unusual phenotype. The effects on *N*-sulfation and growth factor binding were confirmed biochemically. The results indicate that *N*-sulfation or a factor requiring *N*-sulfation regulates primary and secondary branching events in the developing mammary gland. Together with previous work, the data indicate that different stages of ductal branching and lobuloalveolar formation are regulated by distinct sets of heparan sulfate biosynthetic enzymes in an appropriate growth factor context.

The mammary gland develops through the process of branching morphogenesis of the epithelial terminal end bud, which is stimulated by a variety of growth factors and hormones. At birth, the mammary ductal epithelium is a rudimentary structure contained within the fat pad and connected to an exterior nipple. In mice, the gland remains largely quiescent until puberty, and the beginning of the estrous cycle at which time hormones induce rapid ductal epithelial branching leading to the formation of an arborized ductal epithelia by 10–12 weeks of age. Primary epithelial ductal branching and arborization in the developing mammary gland occur through iterative rounds of terminal end bud bifurcation and stalk elongation, whereas secondary (or ductal side) branching occurs along the stalk portions. It is this coordinated growth of the terminal end bud together with secondary branching which ultimately results in filling of the gland with an extensive network of branched ductal epithelia. During pregnancy lobuloalveolar development and terminal differentiation are induced resulting in a mature mammary gland capable of producing milk (for review, see Refs. 1, 2). Thus, development of the mammary gland can be divided into distinct stages depending on the stage of sexual development and reproduction state (3, 4).

Whereas specific heparan sulfate proteoglycans have been implicated in mammary development, recent *in vivo* evidence supports the notion that the heparan sulfate chains (HS)[7] and the pattern of sulfation play a functionally important role in modulating branching morphogenesis of the mammary ductal epithelium (5, 6). Biochemical and *in vitro* cell and organ culture data indicate that the action of HS is dependent upon proper sulfation (7, 8) which is established by the action of a

* This work was supported, in whole or in part, by National Institutes of Health Grants GM33063 and HL57345 (to J. D. E.) and DK57286, DK65831, and DK79784 (to S. K. N.).

[1] Both authors contributed equally to this work.

[2] Portions of this work were included in the Ph.D. dissertations at the University of California San Diego.

[3] Supported by National Research Service Award Grant AI058916.

[4] Present address: Dept. of Pathology and Laboratory Medicine, University of California, Los Angeles, CA 90095.

[5] To whom correspondence may be addressed: Dept. of Cellular and Molecular Medicine, University of California San Diego, 9500 Gilman Dr., La Jolla, CA 92093. Tel.: 858-822-1100; Fax: 858-534--5611; E-mail: jesko@ucsd.edu.

[6] To whom correspondence may be addressed: Dept. of Cellular and Molecular Medicine, Pediatrics, Medicine, and Bioengineering, University of California San Diego, 9500 Gilman Dr., La Jolla, CA 92093. Tel.: 858-822-3482; Fax: 858-822-3483; E-mail: snigam@ucsd.edu.

[7] The abbreviations used are: HS, heparan sulfate; AdCre, cre-recombinase containing adenovirus; Ext1, exotosin-1; Ndst, *N*-deacetylase/*N*-sulfotransferase; Hs2st, heparan sulfate 2-*O*-sulfotransferase; Hs3st, heparan sulfate 3-*O*-sulfotransferase; Hs6st, heparan sulfate 6-*O*-sulfotransferase; MMTV, murine mammary tumor virus.

series of HS biosynthetic enzymes, including members of the *N*-deacetylase/*N*-sulfotransferase (*Ndst*) family, the uronyl C5-epimerase (*Hsglce*), and 2-*O*-sulfotransferase (*Hs2st*), the glucosaminyl 6-*O*-sulfotransferases (*Hs6st*) and 3-*O*-sulfotransferases (*Hs3st*) (31). Because systemic deletion of many of these enzymes results in either embryonic lethality or a lack of defects in mammary gland development or function (9–16), we have investigated the role of HS in mammary ductal epithelial branching morphogenesis by utilizing mammary epithelia-specific deletions of various HS biosynthetic enzymes. For example, tissue-specific inactivation of *Ndst1*, one of only two members of this family expressed in mammary epithelia, had no apparent effect on primary and secondary ductal branching, but selectively perturbed lobuloalveolar development (5). In a subsequent study mammary-specific inactivation of *Ext1* (a subunit of the co-polymerase complex that catalyzes the formation of the HS chain) resulted in a highly penetrant and dramatic defect in primary branching (6). In addition, although inactivation of *Hs2st* (required for 2-*O*-sulfation of uronic acids in HS) resulted in fewer bifurcated terminal end buds, the ductal network was characterized by a marked reduction in secondary/ductal side branches (6). Thus, whereas assembly of the HS chains (mediated by *Ext1*) is key to mammary gland development, selective *O*-sulfation and *N*-sulfation appear to regulate different stages in branching and lobuloalveolar development (5, 6).

Here, we have further analyzed the role of *Ndst* isoforms in the developing mammary gland by co-deletion of *Ndst1* and *Ndst2*, the two members of the *N*-acetylglucosamine *N*-deacetylase/*N*-sulfotransferase family expressed in mammary epithelia. Deletion of both isoforms was found to result in a "hyperbranched" phenotype. Knockouts with clear hyperbranched phenotypes are uncommon. These results highlight the importance of specific HS modifications in the regulation of branching morphogenesis. Taken together with our recent studies (5, 6), the data demonstrate that the pattern of sulfation of the chain determines the extent of ductal epithelial branching (both dichotomous and side branching).

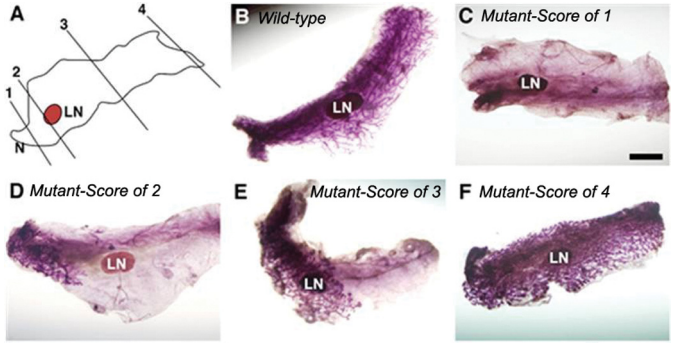

FIGURE 1. ***Ndst*-deficient glands show defects in ductal branching.** Whole mounts of the fourth inguinal mammary glands isolated at 10 weeks. *A*, schematic diagram of the fourth inguinal mouse mammary gland showing the nipple (*N*) and the lymph node (*LN*). *B*, *Ndst1*$^{f/f}$*MMTVCre*$^{-}$*Ndst2*$^{-/-}$ (wild type) gland. *C–F*, *Ndst1*$^{f/f}$*MMTVCre*$^{+}$*Ndst2*$^{-/-}$ (mutant) glands with scores of 1 (*C*), 2 (*D*), 3 (*E*), or 4 (*F*).

TABLE 1
***Ndst1*^{ff}*MMTVCre*$^{-}$, *Ndst1*^{ff}*MMTVCre*$^{-}$*Ndst2*$^{-/-}$, and *Ndst1*^{ff}*MMTVCre*$^{+}$ *Ndst2*$^{-/-}$ glands and the respective growth scores/percentages**

Genotype	Penetrance score			
	1	2	3	4
Ndst1^{ff}*MMTVCre*$^{-}$ (n = 11)	0	0	0	100
Ndst1^{ff}*MMTVCre*$^{-}$*Ndst2*$^{-/-}$ (n = 20)	0	0	0	100
Ndst1^{ff}*MMTVCre*$^{+}$*Ndst2*$^{-/-}$ (n = 79)	18	3	20	59

EXPERIMENTAL PROCEDURES

Generation of Genetic Deletions—All studies were done in accordance with protocols approved by the IACUC and Animal Subjects Committee at the University of California, San Diego. Mice bearing a loxP-flanked allele of *Ndst1* were described previously (5, 9, 32). *Ndst2*-deficient mice were obtained from Dr. L. Kjellen, University of Uppsala, Sweden (22). Cross-breeding was initiated when the *Ndst1*$^{f/f}$ and *Ndst2*$^{-/-}$ mice were backcrossed to C57BL/6 for 4 and 10 generations, respectively. The MMTV Cre line A mice in the 129 background were obtained from Dr. T. Wynshaw-Boris (University of California, San Diego) (33, 34). Only male mice carrying the MMTV Cre allele were used for breeding to avoid deletion of the conditional allele by Cre expression in oocytes. All experiments were done with mice on a mixed background with littermate controls. Over the course of these studies, we did not note any qualitative and quantitative changes of phenotype with further backcrossing of *Ndst1*$^{f/f}$ with C57BL/6 mice.

Cell Culture—Primary mammary epithelia were isolated and cultured following an established protocol (5, 6, 17). Isolated number 3 and 4 glands were digested with 0.2% trypsin and 0.2% collagenase A (Roche Applied Bioscience). Cells were enriched by differential centrifugation. Tissue culture plates were precoated with 100 ml/cm^2 Ham's F12 (Invitrogen) medium containing 20% heat-inactivated fetal bovine serum (FBS) (Atlanta Biologicals, Lawrenceville, GA) and 1 mg/ml fetuin (Sigma). Cells were cultured in Ham's F12 medium containing 10% heat-inactivated FBS, 5 μg/ml insulin, 1 μg/ml hydrocortisone, 5 ng/ml epidermal growth factor, 50 μg/ml gentamycin, 100 units/ml penicillin, and 100 μg/ml streptomycin (all from Sigma). The medium was changed after the 2nd day of culture and subsequently on every other day; cells were cultured for a total of 5–7 days.

Determination of Heparan Sulfate-dependent Ligand Binding to Cells—Isolated primary mammary epithelial cells were incubated with biotinylated ligand (fibroblast growth factor 2 (FGF2)) in Ham's F12 medium (Invitrogen) with 0.5% BSA (Sigma) for 1 h with shaking at 4 °C. Cells were washed twice in PBS and incubated in PBS containing streptavidin-APC for 20 min with shaking at 4 °C. HS-dependent binding of ligand to HS expressed on mammary epithelial cells was determined using flow cytometry as described previously (18).

Transformed mammary ductal epithelial cell lines lacking *Ndst1*, *Ndst2*, or genes in combination were also examined. An adenovirus containing Cre-recombinase (AdCre) was also used to inactivate the *Ndst1*$^{f/f}$ *in vitro* as described (19). AdCre and adenovirus containing green fluorescent protein (AdGFP) were obtained from the Vector Core Development Laboratory at the University of California, San Diego. Cells were treated for 90 min twice over 4 days with 10^8 pfu/ml, washed with PBS, and cultured in normal growth medium. Samples where the biotinylated ligand was omitted were included as negative controls. Flow cytometry using biotinylated probe and streptavidin

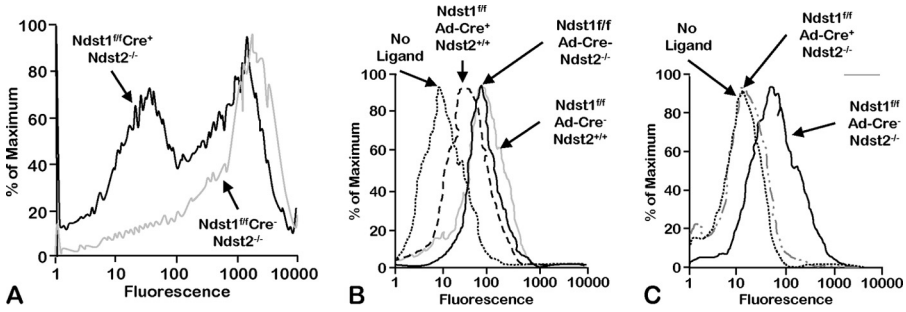

FIGURE 2. ***Ndst*-deficient primary mammary epithelial cells display differences in HS-dependent binding of ligand.** Flow cytometry of either primary mammary ductal epithelial cells (*A*) or transformed mammary epithelial cells (*B* and *C*) treated with biotinylated ligand (FGF2) is shown. *A*, ligand binding to primary ductal epithelial cells isolated from either *Ndst1*$^{f/f}$*MMTVCre*$^{-}$*Ndst2*$^{-/-}$ (*gray line*) or *Ndst1*$^{f/f}$*MMTVCre*$^{+}$*Ndst2*$^{-/-}$ (*black line*). *B* and *C*, ligand binding to transformed mammary epithelial cells transfected with either *Ndst1*$^{f/f}$ or *Ndst1*$^{f/f}$*Ndst2*$^{-/-}$ is shown. Treatment with or without Ad-Cre results in cells bearing either no *Ndst* deletions (*Ndst1*$^{f/f}$*Ad-Cre*$^{-}$*Ndst2*$^{+/+}$), a single deletion in *Ndst2* (*Ndst1*$^{f/f}$*Ad-Cre*$^{-}$*Ndst2*$^{-/-}$), or a double deletion of *Ndst1* and *Ndst2* (*Ndst1*$^{f/f}$*Ad-Cre*$^{+}$*Ndst2*$^{-/-}$). *B*, the absence of *Ndst2* alone (*Ndst1*$^{f/f}$*Ad-Cre*$^{-}$*Ndst2*$^{-/-}$, *solid black line*) has only a minor effect on the binding of the ligand compared with wild type cells (*Ndst1*$^{f/f}$*Ad-Cre*$^{-}$*Ndst2*$^{+/+}$; *solid gray line*). The absence of *Ndst1* alone (*Ndst1*$^{f/f}$*Ad-Cre*$^{+}$*Ndst2*$^{+/+}$; *dashed black line*) reduced ligand binding by ~5-fold. *C*, the absence of both *Ndst1* and *Ndst2* (*Ndst1*$^{f/f}$*Ad-Cre*$^{+}$*Ndst2*$^{-/-}$; *dashed gray line*) results in an almost complete loss of ligand binding, similar to that seen in the absence of ligand (no ligand).

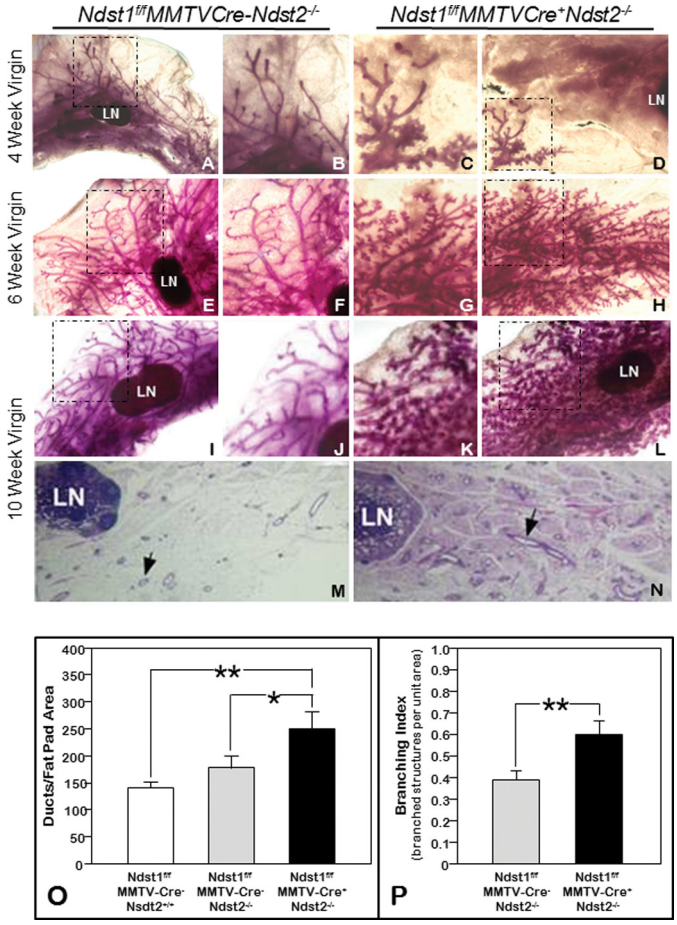

FIGURE 3. ***Ndst*-deficient glands show overabundance of branched epithelial ducts.** *A–L*, whole mounts of the fourth inguinal mammary glands isolated from virgin female mice at 4 (*A–D*), 6 (*E–H*), and 10 (*I–L*) weeks of postnatal development. Mammary glands were isolated from either *Ndst1*$^{f/f}$*MMTVCre*$^{-}$*Ndst2*$^{-/-}$ (*A–B*, *E–F*, *I–J*, *M*) or *Ndst1*$^{f/f}$*MMTVCre*$^{+}$*Ndst2*$^{-/-}$ (*C–D*, *G–H*, *K–L*, *N*) mice. *Insets* (*B*, *C*, *F*, *G*, *J*, and *K*) show higher magnification views of selected areas (*dashed boxes*). *M* and *N*, hematoxylin and eosin-stained histological section of *Ndst1*$^{f/f}$*MMTVCre*$^{-}$*Ndst2*$^{-/-}$ (wild type) (*M*) and *Ndst1*$^{f/f}$*MMTVCre*$^{+}$*Ndst2*$^{-/-}$ (mutant) (*N*) gland at 10 weeks. *LN*, lymph node; *black arrows* point to ducts. *O*, quantitation of mammary ductal epithelium measured as the number of ducts per area of fat pad in *Ndst1*$^{f/f}$*MMTVCre*$^{-}$, *Ndst1*$^{f/f}$*MMTVCre*$^{-}$*Ndst2*$^{-/-}$, and *Ndst1*$^{f/f}$*MMTVCre*$^{+}$*Ndst2*$^{-/-}$ mammary glands. Shown are mean ± S.E. (*error bars*); $n \geq 4$; *, $p \leq 0.05$; **, $p \leq 0.005$. *P*, quantitation of ductal epithelial branching morphogenesis measured as the number of branched structures per unit area (branching index) in *Ndst1*$^{f/f}$*MMTVCre*$^{-}$*Ndst2*$^{-/-}$ and *Ndst1*$^{f/f}$*MMTVCre*$^{+}$*Ndst2*$^{-/-}$ mammary glands. Shown are mean ± S.E.; $n = 4$; **, $p \leq 0.005$.

phycoerythrin-Cy5 showed >10-fold decrease in fluorescence of ~99% of the cells (18).

Mammary Gland Histology—Histological analyses were performed by the Cancer Center Histology Core at the University of California, San Diego. Whole mounts were stained with hematoxylin (20). Hematoxylin and eosin staining of sections was performed by standard procedures.

Heparan Sulfate Analysis—Subconfluent primary mammary epithelial cells were cultured for 48 h in DMEM with the addition of 2 mM glucose, 10% dialyzed FCS, 5 μg/ml insulin, 1 μg/ml hydrocortisone, 5 ng/ml epidermal growth factor and 0.05 mCi/ml [^{3}H]glucosamine. Cell-associated and soluble glycosaminoglycans were isolated and fragmented with nitrous acid, pH 1.5, for *N*-sulfation analysis as described by Bame and Esko (21). Nitrous acid at low pH cleaves the backbone of the polymer at each *N*-sulfated glucosamine unit. The resulting heparan sulfate oligosaccharides were then separated by gel filtration chromatography.

RESULTS

The strategy employed in this study was aimed at eliminating HS *N*-sulfation by targeting both *Ndst* isoforms expressed in mammary glands. *N*-Sulfation is critical to all other subsequent sulfation reactions (5). Mammary-specific inactivation of *Ndst1* was found to only partially reduce sulfation of the HS chains and had no apparent effect on primary branching morphogenesis of the mammary ductal epithelium (5), whereas mammary glands appear essentially normal in *Ndst2*-null animals (22, 23). To further address the role of *N*-sulfation in mammary ductal branching, in this study a more severe reduction in sulfation was performed by inactivating *Ndst1* selectively in mammary ductal epithelia on an *Ndst2*-deficient background. The breeding resulted in littermate pairs of *Ndst1*$^{f/f}$*MMTVCre*$^{+}$*Ndst2*$^{-/-}$ (mutant) mice and *Ndst1*$^{f/f}$*MMTVCre*$^{-}$*Ndst2*$^{-/-}$ (wild type) mice. Mice of both genotypes were obtained at the expected Mendelian frequency.

Deletion of Ndst1 and Ndst2 in the Mammary Gland Alters Growth of the Ductal Epithelium—Whole mounts of the fourth inguinal mammary gland were compared between *Ndst1*$^{f/f}$*MMTVCre*$^{+}$*Ndst2*$^{-/-}$ and *Ndst1*$^{f/f}$*MMTVCre*$^{-}$*Ndst2*$^{-/-}$, mice which revealed a variation of perturbed growth of the ductal network in the mutant (Fig. 1). Because there was a range

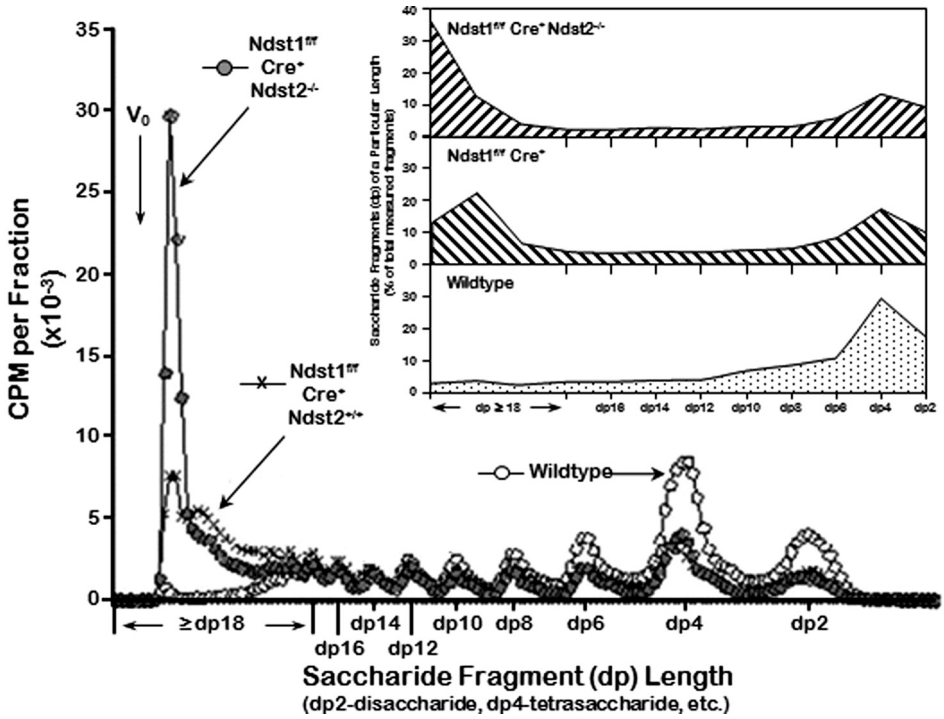

FIGURE 4. **The effect of *Ndst* deletion on *N*-sulfation of HS produced by primary mammary epithelial cells.** Chromatograph of saccharide fragments resulting from the digestion of isolated heparan sulfate by nitrous acid at pH 1.5 is shown. Disaccharides (dp2) represent sequential *N*-sulfated glucosamine residues, whereas tetrasaccharides (dp4) represent *N*-sulfated glucosamines separated by one unmodified glucosamine. Subsequent peaks moving toward the void volume (V_0) represent larger disaccharide fragments with intervening *N*-acetylated glucosamine residues. Wild type (*open circles*) mammary epithelia produce extensively *N*-sulfated HS resulting in small oligosaccharide fragments (major peak fractions are from dp2 to dp6 (*inset*)) whereas single *Ndst1* deletions ($Ndst1^{f/f}Ndst2^{+/+}MMTVCre^{+}$ epithelia (×)) and *Ndst1/Ndst2* double deletions ($Ndst1^{f/f}Ndst2^{-/-}MMTVCre^{+}$ epithelia (*filled circles*)) generate much less sulfated HS resulting in larger oligosaccharide fragments with ~50% of normal *N*-sulfation (≥dp18, *inset*).

of perturbed growth, a scoring system based on the extent of ductal epithelial growth, similar to that used in our recent study on the inactivation of *Ext1* and *Hs2st* (as well as cmet), was utilized to quantify the effect of loss of both *Ndst1* and *Ndst2* ductal branching 10–12 weeks postpartum (6). In this system, glands are given a score from 1 to 4 based on the extent of ductal growth in relation to the nipple, lymph node, and the end of the fat pad. Briefly, the absence of ductal growth resulted in a score of 1, ducts that grew from the nipple but stopped prior to the lymph node were scored as a 2. Ductal trees that progressed past the lymph node but halted before the end of the fat pad distal to the nipple received a score of 3. Growth that completely filled the fat pad received a score of 4. Using this system, $Ndst1^{f/f}MMT\ Cre^{-}Ndst2^{-/-}$ (wild type) mice all exhibited a wild type mammary ductal growth score (Table 1). 18% of $Ndst1^{f/f}MMTVCre^{+}Ndst2^{-/-}$ mice were devoid of any ductal growth. 23% of $Ndst1^{f/f}MMTVCre^{+}Ndst2^{-/-}$ glands showed growth that stopped at a score of 2 or 3, whereas 59% of the mutant glands exhibited an apparent wild type phenotype (Table 1). Animals aged to 9 months showed a similar distribution of growth (data not shown).

To examine the efficiency of Cre inactivation and to gain further insight into the role of each *Ndst*, the binding properties of HS remaining on the cells were assessed by flow cytometry, using biotinylated FGF as a ligand/probe as described (18). Binding to either primary mammary ductal epithelial cells (Fig. 2*A*) or transformed mammary epithelial cell lines (Fig. 2, *B* and *C*) were quantified by flow cytometry. The cell surface HS in $Ndst1^{f/f}MMTVCre^{+}Ndst2^{-/-}$ glands (Fig. 2*A*, *black line*) was compared with that found in $Ndst1^{f/f}MMTVCre^{-}Ndst2^{-/-}$ glands (Fig. 2*A*, *gray line*). Isolated epithelia from these animals necessarily had to come from glands that produced epithelia (a score of 2 or higher). Flow cytometry revealed two distinct cell populations in the $Ndst1^{f/f}MMTVCre^{+}Ndst2^{-/-}$ glands. One bound at the level of $Ndst1^{f/f}MMTVCre^{-}Ndst2^{-/-}$ cells whereas the other population showed a significant decrease in binding. This finding suggested that there was an incomplete deletion of *Ndst1* by Cre-recombinase, resulting in variable sulfation and the observed inconsistent growth of the ductal epithelium within the fat pad.

To examine this possibility further, transformed mammary epithelial cells were used to test the effect of deletion of the *Ndsts* on ligand binding using the flow cytometry assay. $Ndst1^{f/f}Ndst2^{-/-}$ cells, cultured in the absence of AdCre, exhibited only a minor reduction in binding (Fig. 2*B*, *solid black line*) compared with $Ndst1^{f/f}Ndst2^{+/+}$ cells (Fig. 2*B*, *gray line*). $Ndst1^{-/-}Ndst2^{+/+}$ cells, in which *Ndst1* was excised in the presence of AdCre, however, were found to bind 5-fold less biotinylated probe (Fig. 2*B*, *dashed line*). Combining the mutations ($Ndst1^{-/-}Ndst2^{-/-}$) led to a virtually complete loss of binding (Fig. 2*C*, *dashed gray line*), a level comparable with that observed in the absence of ligand (Fig. 2*C*, *dotted line*). This finding is consistent with a complete lack *N*-sulfation in this cell line.[8] No compensatory change in *Ndst3* or *Ndst4* expression was detected by PCR analysis (data not shown).

[8] J. McArthur and J. Esko, unpublished results.

Ndst-deficient Ducts Display an Apparent Overabundance of Branched Ductal Epithelia and Cellular Chimerism in the Level of Sulfated Cell Surface Heparan Sulfate—A closer examination of Ndst1$^{f/f}$*MMTVCre*$^{+}$*Ndst2*$^{-/-}$ mutant glands revealed an apparent overabundance of pubertal ductal epithelial growth and apparent branched structures. Examination of whole mounts from the start of pubertal mammary development (4 weeks) demonstrated clear differences in the development of the ductal epithelium (Fig. 3). *Ndst1*$^{f/f}$*MMTVCre*$^{-}$*Ndst2*$^{-/-}$ littermate pairs showed regular spacing between ducts in whole mounts (Fig. 3); in contrast, *Ndst1*$^{f/f}$*MMTVCre*$^{+}$*Ndst2*$^{-/-}$ glands showed a marked increase in ductal epithelium by whole mount accompanied by the appearance of an abundance of side branches (Fig. 3). As described above, the development of these branches was apparent from the outset of mammary gland development and continued throughout development leading to the formation of mammary gland fat pads filled with highly branched structures (Fig. 3). Examination of histological sections confirmed this finding (compare Fig. 3, *M* and *N*; *black arrows* point to ducts). This result was quantified by comparing the total number of ducts in a section per area of the fat pad, and there is clearly a significant increase in the amount of ductal epithelia in the double mutant mammary glands (Fig. 3*O*). In addition, the extent of ductal branching was also quantified at 12 weeks of mammary gland development. In this analysis, the number of branched structures per unit area of the mammary gland (*i.e.* branching index) was determined (Fig. 3*P*). The data indicate that *Ndst*-deficient animals display >1.5-fold increase in the number of branched structures per unit area compared with wild type animals (Fig. 3). Importantly, the increased branching phenotype was apparent in *Ndst1*$^{f/f}$*MMTVCre*$^{+}$*Ndst2*$^{-/-}$ mutant glands, regardless of the growth score (*i.e.* 1–4) (Fig. 1 and Table 1) or postnatal age (Fig. 3).

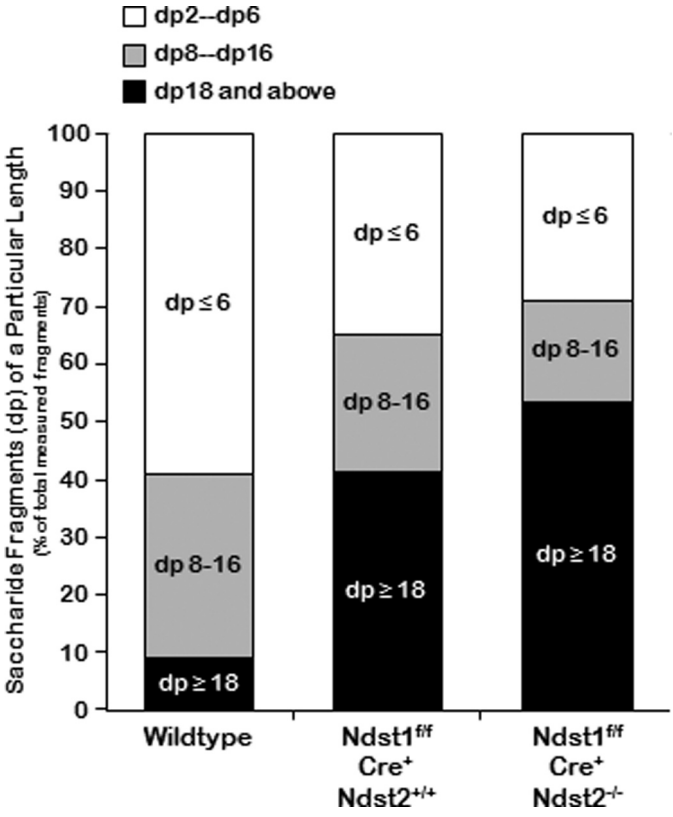

FIGURE 5. ***Stacked bar graphs*** **illustrating the amount of the various saccharide fragment lengths as a percentage of the entire volume applied to the column.** In wild type cells the amount of disaccharide (dp2), tetrasaccharide (dp4), and hexasaccharide (dp6) represents almost 60% of the total, whereas octasaccharide to hexadecasaccharide fragments (dp8–16) represent ~30%, and dp ≥18 represent <10% of the total. In mutant cells the amount of dp8–16 oligosaccharides decreases progressively, but the amount of ≥dp18 accumulates, accounting for 45–55% of the total amount of oligosaccharide fragments.

Deletion of Ndst1 and Ndst2 in Mammary Gland Alters HS Sulfation—To confirm that deletion *Ndst1* and *Ndst2* reduced *N*-sulfation of HS in the mammary epithelia the degree of *N*-sulfation in *Ndst1*$^{f/f}$*MMTVCre*$^{+}$*Ndst2*$^{-/-}$ mammary epithelial cells was analyzed (Fig. 4, *filled circles*). Low pH nitrous acid was used to fragment the polymer adjacent to sites of *N*-sulfation. In this analysis, highly sulfated domains containing alternating *N*-sulfated glucosamine residues are fragmented into disaccharides, whereas regions lacking *N*-sulfation yield longer oligosaccharides whose size depends on the spacing of *N*-sulfated units. In other words, a highly *N*-sulfated HS would be expected to fragment into numerous small oligosaccharide fragments, whereas a sparsely *N*-sulfated HS would result in a greater percentage of large oligosaccharide fragments.

As expected, in wild type cells, almost 60% of the oligosaccharide fragments isolated from the column were either disaccharides (dp2), tetrasaccharides (dp4), or hexasaccharides (dp6) (Fig. 5, dp≤6). However, deletions of either *Ndst1* or a combination of *Ndst1* and *Ndst2* led to the accumulation of octadecasaccharide and larger fragments (dp≥18) (Fig. 5) and a reduction in the percentage of smaller oligosaccharide fragments (Fig. 5). Although incomplete deletion of *Ndst1 in vivo* may have occurred due to incomplete penetrance of the Cre-recombinase expression (Figs. 1 and 2), the overall patterns are consistent with altered structure of the HS in the tissue.

DISCUSSION

In this study, we demonstrate a relatively unusual so-called "hyperbranched" phenotype in developing mouse mammary gland by interfering with proper *N*-sulfation of HS by deletion

TABLE 2

Effects of deletions of genes involved in HS initiation, polymerization, and sulfation on mammary gland branching and differentiation

Genes are listed in the order of heparan sulfate modifications catalyzed during GAG assembly and sulfation: *Ext→Ndst→Hsglce→Hs2st→Hs6st→Hs3st.*

Deleted gene	Phenotype	Stage of mammary gland development affected			Reference
		Primary branching	Secondary branching	Lobuloalveolar development	
Ext	Lack of branching ductal epithelium	X			6
Ndst1	Lack of lobuloalveolar expansion			X	5
Ndst2	Mild increase in branching	X	X		
Ndst1/Ndst2	Hyperbranching	X	X		
Hs2st	Decrease in secondary/ductal side branching		X		6

of *Ndst2* and *Ndst1* (Figs. 1–3). Deletion of *Ndst2* alone caused a mild increase in branched structures (data not shown), which became exaggerated and quantitatively significant, after *Ndst*1 was also deleted. Both primary and secondary branching appeared to be affected.

Postnatal mammary gland branching morphogenesis begins with formation of a bud, which then undergoes primary branching and formation of terminal end buds, followed by secondary or side branching, followed by lobuloalveolar development (and terminal differentiation with milk production) during pregnancy. We have previously demonstrated that deletion of *Ext1*, which is necessary for co-polymerization of HS chains, prevents primary branching of the mammary gland ductal system (6). In contrast, deletion of *Hs2st*, which is responsible for selective 2-*O*-sulfation of uronic acids, affects secondary or side branching as well as terminal end bud formation (6). Deletion of *Ndst1* alone, on the other hand, does not substantially affect branching but causes a dramatic focal defect in lobuloalveolar development (5). Here, we have shown that *Ndst2* deletion in combination with the *Ndst1* mammary epithelia-specific deletion increases primary and secondary branching.

In vivo branching phenotypes due to deletion of HS biosynthetic enzymes have been difficult to identify in many branching organs. This is partly due to the fact that many of the systemic knockouts of HS biosynthetic enzymes suffer from early embryonic lethality. In the developing kidney, the situation is somewhat different since, in some mutant animals, lethality occurs subsequent to at least the early stages of kidney morphogenesis. For example, null mutations in C-5 epimerase or Hs2st result in renal agenesis which, at least in the case of Hs2st, appears to be due to a failure of epithelial branching morphogenesis (11, 12). Recent studies utilizing *ex vivo* culture of the mouse embryonic kidney, as well as its progenitor tissues, have demonstrated a clear role for Hs2st and Hs6st as modulators of epithelial branching morphogenesis, albeit due to effects on different growth factor-HS interactions critical to kidney development (26, 27). However, in the mammary gland, through the use of selective tissue-specific gene deletions, we have been able to demonstrate that heparan sulfation itself, as well as selective *N*- and *O*-sulfation of HS occurring through the action of different sets of HS biosynthetic enzymes (and their isoforms) regulate distinct aspects of branching morphogenesis in the developing mammary gland (Table 2).

Together, these seem to be the clearest *in vivo* examples so far of how individual stages of epithelial branching morphogenesis depend upon the steps in HS biosynthesis. Moreover, this finding is consistent with the idea that selective HS-growth factor interactions help "switch" the stages of branching in the organogenesis of epithelial tissues (5, 6, 24–30). If correct, the delineation of stage-specific growth factors that interact with selectively sulfated HS and facilitate the progression of the stages of mammary gland branching morphogenesis should be a fertile area for future research.

REFERENCES

1. Sternlicht, M. D. (2006) Key stages in mammary gland development: the cues that regulate ductal branching morphogenesis. *Breast Cancer Res.* **8,** 201
2. Sternlicht, M. D., Kouros-Mehr, H., Lu, P., and Werb, Z. (2006) Hormonal and local control of mammary branching morphogenesis. *Differentiation* **74,** 365–381
3. Imagawa, W., Bandyopadhyay, G. K., and Nandi, S. (1990) Regulation of mammary epithelial cell growth in mice and rats. *Endocr. Rev.* **11,** 494–523
4. Sunil, N., Srinivasan, N., Aruldhas, M. M., and Govindarajulu, P. (2000) Impact of oestradiol and progesterone on the glycosaminoglycans and their depolymerizing enzymes of the rat mammary gland. *Acta Physiol. Scand.* **168,** 385–392
5. Crawford, B. E., Garner, O. B., Bishop, J. R., Zhang, D. Y., Bush, K. T., Nigam, S. K., and Esko, J. D. (2010) Loss of the heparan sulfate sulfotransferase, *Ndst1*, in mammary epithelial cells selectively blocks lobuloalveolar development in mice. *PLoS One* **5,** e10691
6. Garner, O. B., Bush, K. T., Nigam, K. B., Yamaguchi, Y., Xu, D., Esko, J. D., and Nigam, S. K. (2011) Stage-dependent regulation of mammary ductal branching by heparan sulfate and HGF-cMet signaling. *Dev. Biol.* **355,** 394–403
7. Silberstein, G. B., and Daniel, C. W. (1982) Glycosaminoglycans in the basal lamina and extracellular matrix of the developing mouse mammary duct. *Dev. Biol.* **90,** 215–222
8. Gordon, J. R., and Bernfield, M. R. (1980) The basal lamina of the postnatal mammary epithelium contains glycosaminoglycans in a precise ultrastructural organization. *Dev. Biol.* **74,** 118–135
9. Grobe, K., Inatani, M., Pallerla, S. R., Castagnola, J., Yamaguchi, Y., and Esko, J. D. (2005) Cerebral hypoplasia and craniofacial defects in mice lacking heparan sulfate *Ndst1* gene function. *Development* **132,** 3777–3786
10. Ringvall, M., Ledin, J., Holmborn, K., van Kuppevelt, T., Ellin, F., Eriksson, I., Olofsson, A. M., Kjellen, L., and Forsberg, E. (2000) Defective heparan sulfate biosynthesis and neonatal lethality in mice lacking *N*-deacetylase/*N*-sulfotransferase-1. *J. Biol. Chem.* **275,** 25926–25930
11. Li, J. P., Gong, F., Hagner-McWhirter, A., Forsberg, E., Abrink, M., Kisilevsky, R., Zhang, X., and Lindahl, U. (2003) Targeted disruption of a murine glucuronyl C5-epimerase gene results in heparan sulfate lacking L-iduronic acid and in neonatal lethality. *J. Biol. Chem.* **278,** 28363–28366
12. Bullock, S. L., Fletcher, J. M., Beddington, R. S., and Wilson, V. A. (1998) Renal agenesis in mice homozygous for a gene trap mutation in the gene encoding heparan sulfate 2-sulfotransferase. *Genes Dev.* **12,** 1894–1906
13. Habuchi, H., Nagai, N., Sugaya, N., Atsumi, F., Stevens, R. L., and Kimata, K. (2007) Mice deficient in heparan sulfate 6-*O*-sulfotransferase-1 exhibit defective heparan sulfate biosynthesis, abnormal placentation, and late embryonic lethality. *J. Biol. Chem.* **282,** 15578–15588
14. Izvolsky, K. I., Lu, J., Martin, G., Albrecht, K. H., and Cardoso, W. V. (2008) Systemic inactivation of *Hs6st1* in mice is associated with late postnatal mortality without major defects in organogenesis. *Genesis* **46,** 8–18
15. HajMohammadi, S., Enjyoji, K., Princivalle, M., Christi, P., Lech, M., Beeler, D., Rayburn, H., Schwartz, J. J., Barzegar, S., de Agostini, A. I., Post, M. J., Rosenberg, R. D., and Shworak, N. W. (2003) Normal levels of anticoagulant heparan sulfate are not essential for normal hemostasis. *J. Clin. Invest.* **111,** 989–999
16. Hasegawa, H., and Wang, F. (2008) Visualizing mechanosensory endings of TrkC-expressing neurons in HS3ST-2-hPLAP mice. *J. Comp. Neurol.* **511,** 543–556
17. Pullan, S., Wilson, J., Metcalfe, A., Edwards, G. M., Goberdhan, N., Tilly, J., Hickman, J. A., Dive, C., and Streuli, C. H. (1996) Requirement of basement membrane for the suppression of programmed cell death in mammary epithelium. *J. Cell Sci.* **109,** 631–642
18. Schuksz, M., Fuster, M. M., Brown, J. R., Crawford, B. E., Ditto, D. P., Lawrence, R., Glass, C. A., Wang, L., Tor, Y., and Esko, J. D. (2008) Surfen, a small molecule antagonist of heparan sulfate. *Proc. Natl. Acad. Sci. U.S.A.* **105,** 13075–13080
19. Li, M., Wagner, K. U., and Furth, P. A. (2000) in *Methods in Mammary Gland Biology and Breast Cancer Research* (Asch, B. B., ed) pp. 233–244, Kluwer Academic, New York
20. Ip, M. M., and Asch, B. B. (2000) Introduction: an histology atlas of the rodent mammary gland and human breast during normal postnatal devel-

opment and in cancer. *J. Mammary Gland Biol. Neoplasia* **5,** 117–118
21. Bame, K. J., and Esko, J. D. (1989) Undersulfated heparan sulfate in a Chinese hamster ovary cell mutant defective in heparan sulfate *N*-sulfotransferase. *J. Biol. Chem.* **264,** 8059–8065
22. Forsberg, E., Pejler, G., Ringvall, M., Lunderius, C., Tomasini-Johansson, B., Kusche-Gullberg, M., Eriksson, I., Ledin, J., Hellman, L., and Kjellén, L. (1999) Abnormal mast cells in mice deficient in a heparin-synthesizing enzyme. *Nature* **400,** 773–776
23. Humphries, D. E., Wong, G. W., Friend, D. S., Gurish, M. F., Qiu, W. T., Huang, C., Sharpe, A. H., and Stevens, R. L. (1999) Heparin is essential for the storage of specific granule proteases in mast cells. *Nature* **400,** 769–772
24. Nigam, S. K., and Shah, M. M. (2009) How does the ureteric bud branch? *J. Am. Soc. Nephrol.* **20,** 1465–1469
25. Sampogna, R. V., and Nigam, S. K. (2004) Implications of gene networks for understanding resilience and vulnerability in the kidney branching program. *Physiology* **19,** 339–347
26. Shah, M. M., Sakurai, H., Gallegos, T. F., Sweeney, D. E., Bush, K. T., Esko, J. D., and Nigam, S. K. (2011) Growth factor-dependent branching of the ureteric bud is modulated by selective 6-*O*-sulfation of heparan sulfate. *Dev. Biol.* **356,** 19–27
27. Shah, M. M., Sakurai, H., Sweeney, D. E., Gallegos, T. F., Bush, K. T., Esko, J. D., and Nigam, S. K. (2010) *Hs2st*-mediated kidney mesenchyme induction regulates early ureteric bud branching. *Dev. Biol.* **339,** 354–365
28. Shah, M. M., Sampogna, R. V., Sakurai, H., Bush, K. T., and Nigam, S. K. (2004) Branching morphogenesis and kidney disease. *Development* **131,** 1449–1462
29. Shah, M. M., Tee, J. B., Meyer, T., Meyer-Schwesinger, C., Choi, Y., Sweeney, D. E., Gallegos, T. F., Johkura, K., Rosines, E., Kouznetsova, V., Rose, D. W., Bush, K. T., Sakurai, H., and Nigam, S. K. (2009) The instructive role of metanephric mesenchyme in ureteric bud patterning, sculpting, and maturation and its potential ability to buffer ureteric bud branching defects. *Am. J. Physiol. Renal. Physiol.* **297,** F1330–1341
30. Steer, D. L., Shah, M. M., Bush, K. T., Stuart, R. O., Sampogna, R. V., Meyer, T. N., Schwesinger, C., Bai, X., Esko, J. D., and Nigam, S. K. (2004) Regulation of ureteric bud branching morphogenesis by sulfated proteoglycans in the developing kidney. *Dev. Biol.* **272,** 310–327
31. Esko, J. D., and Lindahl, U. (2001) Molecular diversity of heparan sulfate. *J. Clin. Invest.* **108,** 169–173
32. Forsberg, E., Pejler, G., Ringvall, M., Lunderius, C., Tomasini-Johansson, B., Kusche-Gullberg, M., Eriksson, I., Ledin, J., Hellman, L., and Kjellen, L. (1999) Abnormal mast cells in mice deficient in haparing-synthesizing enzyme. *Nature* **400,** 773–776
33. Wagner, K. U., Wall, R. J., St-Onge, L., Gruss, P., Wynshaw-Boris, A., Garrett, L., Li, M., Furth, P. A., and Hennighausen, L. (1997) Cre-mediated gene deletion in the mammary gland. *Nucleic Acids Res.* **25,** 4323–4330
34. Wagner, K. U., McAllister, K., Ward, T., Davis, B., Wiseman, R., and Hennighausen, L. (2001) Spatial and temporal expression of the Cre gene under the control of the MMTV-LTR in different lines of transgenic mice. *Transgenic Res.* **10,** 545–553